Blind Identification and Equalization of MC-CDMA Systems Using Higher Order Cumulants

Mohammed ZIDANE, Said SAFI, Mohamed SABRI, Ahmed BOUMEZZOUGH, and Miloud FRIKEL

***Abstract*—In this work we propose an algorithm based on fourth order cumulants for identification of the linear system (Finite Impulse Response (FIR)) with Non Minimum Phase (NMP) excited by non-Gaussian sequences, independent identically distributed (i.i.d). In order to test its efficiency, we have compared with the Safi et al. algorithm, for that we considered three practical frequency-selective fading channel, called Broadband Radio Access Network (BRAN A, BRAN B, and BRAN D), normalized for MC−CDMA systems. In the part of MC−CDMA, we use the zero forcing (ZF) and the minimum mean square error (MMSE) equalizers to perform our algorithms. The simulation results show that the bit error rate (BER) performances of the downlink MC−CDMA systems, using proposed algorithm (AlgoZ) is more accurate compared with the results obtained with the Safi et al. (Alg−CUM) algorithm.**

***Keywords*—NMP channel, Blind System Identification and Equalization, Higher Order Statistics, MC−CDMA systems.**

I. Introduction

In this work, identification of a finite impulse response (FIR) linear system driven by a non gaussian in noisy environment is considered. When the process is Gaussian, the autocorrelation sequence of the observed process is used to identify the system, but the autocorrelation sequence is insensitive to the phase characteristics of the system, and a non minimum phase system cannot be identified correctly using the autocorrelation sequence [1]. Further, the autocorrelation sequence fails to provide a complete statistical description for a non Gaussian process [2], it was shown that consistent estimates of the parameters of any FIR system can be obtained by using higher order statistics or cumulants of the observed process [2],[3]. This is because the higher order cumulants preserve the phase characteristics, unlike the autocorrelation sequence.

Many algorithms exist, in the literature for the identification of the non-minimum phase FIR system using higher order cumulants [2],[4],[8],[9],[10].

In this paper, we have, principally, focussed in channels impulse response estimation with non minimum phase and selective frequency such as: BRAN A, BRAN B, and BRAN D normalized for MC-CDMA systems. In most wireless environments, there are many obstacles in the channels, such as buildings, mountains and walls between the transmitter and the receiver. Reections from these obstacles cause many different propagation paths. The problem encountered in communication is the synchronization between the transmitter and the receiver, due to the echoes and reection between the transmitter and the receiver. To solve the problem of phase estimation we will use, the Higher order cumulants (HOC) to test whats the robustness of those techniques if the channel is affected by a gaussian noise.

In this paper, we propose an algorithm based, only, on fourth order cumulants. In order to test its efciency, we have compared with the Safi et al. algorithm [2], for that we considered three practical frequency-selective fading channel, called Broadband Radio Access Network (BRAN A, BRAN B, and BRAN D), normalized by the European Telecommunications Standards Institute (ETSI) in [12] and [13]. The simulation results show that the bit error rate (BER) performances of the downlink MC-CDMA systems (transmission from the base station to the mobile systems), using proposed algorithm (AlgoZ) is more accurate compared with the results obtained with the Safi et al (Alg−CUM) algorithm.

II. Preliminaries and problem statement

A. Model and assumptions

We consider the single-input single-output (SISO) model (figure 1) of the Finite Impulse Response (FIR) system described by the following relationships:

Noise free case :

$$y(k) = \sum_{i=1}^{q} x(i)h(k-i) \tag{1}$$

With noise :

$$r(k) = y(k) + n(k) \tag{2}$$

Where $x(i)$ is the input sequence, is the impulse response coefficients, q is the order of FIR system, is $r(k)$ the mesured output of system and $n(k)$ is the noise sequence.

In order to simplify the construction of the algorithm we

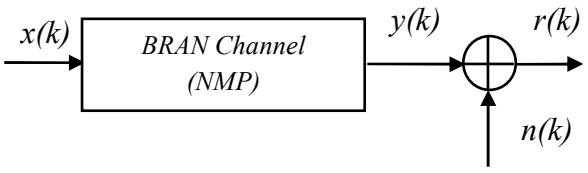

Fig. 1. Channel model

assume that: The input sequence, $x(k)$, is independent and

M. ZIDANE and S. SAFI are with the Department of Mathematics and Informatics, Polydisciplinary Faculty, Sultan Moulay Slimane University, Morocco.

M. SABRI, A. BOUMEZZOUGH are with Department of Physics, Faculty of Sciences and technology, Sultan Moulay Slimane University, Morocco.

M. FRIKEL is with GREYC laboratory, ENSICAEN School, Caen University, France.

identically distributed $(i.i.d)$ zero mean, and non-Gaussian. The system is causal and truncated, i.e. $h(k) = 0$ for $i < 0$ and $i > q$, where $h(0) = 1$. The system order q is known. The measurement noise sequence $n(k)$ is assumed zero mean, i.i.d, Gaussian and independent of $x(k)$ with unknown variance.

B. Basic relationships

In this section, we present the general fundamental relations which permit to identify the FIR linear systems using Higher Order Cumulants (HOC).

The mth order cumulants of the $y(n)$ can be expressed as a function of impulse response coefficients $h(i)$ as follows [2],[4],[7],[9],[10]:

$$C_{my}(t_1, t_2, ..., t_{m-1}) = \xi_{mx} \sum_{i=0}^{q} h(i)h(i+t_1)...h(i+t_{m-1}). \tag{3}$$

Where ξ_{mx} represents the m^{th} order cumulants of the excitation signal $x(i)$ at origin.
If $m = 2$ into Eq. (3) we obtain the second order cumulant (AutoCorrelation Function (ACF)):

$$C_{2y}(t) = \xi_{2x} \sum_{i=0}^{q} h(i)h(i+t) \tag{4}$$

For $m = 4$, Eq. (3) becomes:

$$C_{4y}(t_1, t_2, t_3) = \xi_{4x} \sum_{i=0}^{q} h(i)h(i+t_1)h(i+t_2)h(i+t_3). \tag{5}$$

The Fourier transforms of the 2^{nd} and 4^{rd} order cumulants are given respectively by the following equations [6],[11]:

$$\begin{aligned} S_{2y}(\omega) = TF\{C_{2y}(t)\} &= \xi_{2x} \sum_{i=0}^{q} \sum_{t=-\infty}^{+\infty} h(i)h(i+t) \exp(-j\omega t) \\ &= \xi_{2x} H(-\omega)H(\omega) \end{aligned} \tag{6}$$

With

$$H(\omega) = \sum_{i=0}^{+\infty} h(i) \exp(-j\omega t) \tag{7}$$

$$\begin{aligned} S_{4y}(\omega_1, \omega_2, \omega_3) &= TF\{C_{4y}(t_1, t_2, t_3)\} \\ &= \xi_{4x} H(-\omega_1 - \omega_2 - \omega_3)H(\omega_1)H(\omega_2)H(\omega_3) \end{aligned} \tag{8}$$

So, if we take $\omega = \omega_1 + \omega_2 + \omega_3$, the equation (8) becomes:

$$S_{2y}(\omega_1 + \omega_2 + \omega_3) = \xi_{2x} H(-\omega_1 - \omega_2 - \omega_3)H(\omega_1 + \omega_2 + \omega_3) \tag{9}$$

Then, from the Eqs, (8) and (9) we construct a relationship between the spectrum, the bispectrum and the parameters of the output system:

$$S_{4y}(\omega_1, \omega_2, \omega_3)H(\omega_1+\omega_2+\omega_3) = \mu H(\omega_1)H(\omega_2)H(\omega_3)S_{2y}(\omega_1+\omega_2+\omega_3) \tag{10}$$

With
$\mu = \frac{\xi_{4x}}{\xi_{2x}}$
The inverse Fourier transform of the Eq. (10) is:

$$\sum_{i=0}^{q} C_{4y}(t_1-i, t_2-i, t_3-i)h(i) = \mu \sum_{i=0}^{q} h(i)h(t_2-t_1+i)h(t_3-t_1+i)C_{2y}(t_1-i). \tag{11}$$

Based on the relationship (11) we can develop the following algorithm based on the Higher Order Statistics (HOC).

III. Proposed algorithm: AlgoZ

if we take $t_1 = t_2$ into Eq. (11) we obtain:

$$\sum_{i=0}^{q} C_{4y}(t_1-i, t_1-i, t_3-i)h(i) = \mu \sum_{i=0}^{q} h(i)h(i)h(t_3-t_1+i)C_{2y}(t_1-i). \tag{12}$$

If we use the ACF property of the stationary process such as $C_{2y(t)} \neq 0$ only for $-q \leq t \leq q$ and vanishes elsewhere if we suppose that $t_1 = -q$ the Eq. (11) becomes:

$$\sum_{i=0}^{q} C_{4y}(-q-i, -q-i, t_3-i)h(i) = \mu h^2(0)h(t_3+q)C_{2y}(-q) \tag{13}$$

If we suppose that the system is causal and truncated (i.e. $h(i) = 0$ for $i < 0$ and $i > q$), the choice of t_3 imposes that $t_3 \geq -q$. So, this implies $0 \leq t_3 + q \leq q$. For this reason, we have $t_3 = -q, -q + 1, , 0$.
Else if we take $t_1 = t_3 = -q$ into the Eq. (12), we obtain the following equation:

$$\sum_{i=0}^{q} C_{4y}(-q-i, -q-i, -q-i)h(i) = \mu \sum_{i=0}^{q} h(i)h(i)h(i)C_{2y}(-q-i). \tag{14}$$

According to the ACF property the relation (14) becomes:

$$C_{4y}(-q, -q, -q)h(0) = \mu h^3(0)C_{2y}(-q) \tag{15}$$

With $h(0) = 1$ we obtain:

$$C_{4y}(-q, -q, -q) = \mu C_{2y}(-q) \tag{16}$$

So, we based on Eq. (16) for eliminating $C_{2y}(-q)$ in Eq. (13), we obtain the equation constituted of only the fourth order cumulants:

$$\sum_{i=0}^{q} C_{4y}(-q-i, -q-i, t_3-i)h(i) = h(t_3+q)C_{4y}(-q, -q, -q) \tag{17}$$

Where $t_3 = -q, -q + 1, ..., 0$. The system of Eq. (17) can be written under the matrix form as follows:

$$\begin{pmatrix} C_{4y}(-q-1,-q-1,-q-1) & ... & C_{4y}(-2q,-2q,-2q) \\ C_{4y}(-q-1,-q-1,-q)-\alpha & ... & C_{4y}(-2q,-2q,-2q+1) \\ . & . & . \\ . & . & . \\ . & . & . \\ C_{4y}(-q-1,-q-1,-1) & ... & C_{4y}(-2q,-2q,-q)-\alpha \end{pmatrix}$$

$$\times \begin{pmatrix} h(1) \\ . \\ . \\ . \\ h(i) \\ . \\ . \\ . \\ h(q) \end{pmatrix} = \begin{pmatrix} 0 \\ -C_{4y}(-q,-q,-q+1) \\ . \\ . \\ . \\ . \\ -C_{4y}(-q,-q,0) \end{pmatrix} \quad (18)$$

Where
$\alpha = C_{4y}(-q,-q,-q)$
Or in more compact form, the Eq. (18) can be written as follows:

$$Mh_e = d \quad (19)$$

With M the matrix of size $(q+1,q)$ elements, h a column vector of size $(q,1)$ and d is a column vector of size $(q+1,1)$. The Least Square (LS) solution of the system of equation (19) is given by:

$$\widehat{h}_e = (M^T M)^{-1} M^T d \quad (20)$$

IV. Safi et al Algorithm: Alg-CUM [2]

Safi et al.[2] demonstrates that the coefficients $h(j)$for an FIR system can be obtained by the relationship, based on three order cumulants following:

$$\sum_{i=0}^{q} C_{3y}(-q-i,t_2-i)h(i) = C_{3y}(-q,-q)h(t_2+q) \quad (21)$$

With $t_2 = -q,...,0$ The system of Eq. (20) can be written under the matrix form as follows:

$$\begin{pmatrix} C_{3y}(-q-1,-q-1) & ... & C_{3y}(-2q,-2q) \\ C_{3y}(-q-1,-q)-\alpha & ... & C_{3y}(-2q,-2q+1) \\ . & . & . \\ . & . & . \\ . & . & . \\ C_{3y}(-q-1,-1) & ... & C_{3y}(-2q,-q)-\alpha \end{pmatrix}$$

$$\times \begin{pmatrix} h(1) \\ . \\ . \\ . \\ h(i) \\ . \\ . \\ . \\ h(q) \end{pmatrix} = \begin{pmatrix} 0 \\ -C_{3y}(-q,-q+1) \\ . \\ . \\ . \\ . \\ -C_{3y}(-q,0) \end{pmatrix} \quad (22)$$

Where
$\alpha = C_{3y}(-q,-q)$
The Eq. (22) can be written as follows:

$$Mh_e = d \quad (23)$$

Where M is the matrix of size $(q+1)\times(q)$ elements, h_e is a column vector constituted by the unknown impulse response parameters $h(k) = k = 0,...,q$ and d is a column vector of size $(q+1)$ as indicated in the Eq. (23).

The least squares (LS) solution of the system of Eq. (23), will be written under the following form

$$\widehat{h}_e = (M^T M)^{-1} M^T d \quad (24)$$

V. Application: identification and equalization of MC-CDMA system

The MC−CDMA modulator spreads the data of each user in frequency domain, the complex symbol a_j of each user j is, firstly, multiplied by each chips $c_(j,k)$ of spreading code, and then applied to the modulator of multicarriers. Each subcarrier transmits an element of information multiplied by a code chip of that subcarrier. In figure 2 we have represented the principle of MC−CDMA modulator:

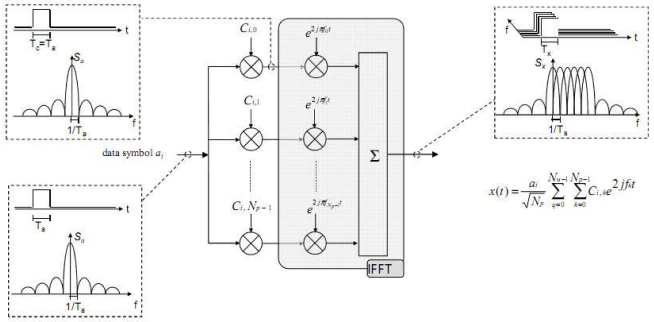

Fig. 2. Principle of MC−CDMA modulator the symbol a_j of each user j

A. MC−CDMA Transmitter

Figure 3 explains the principle of the transmitter for down-link MC−CDMA systems. The MC−CDMA signal is given by

$$x(t) = \frac{a_i}{\sqrt{N_p}} \sum_{q=0}^{N_u-1} \sum_{k=0}^{N_p-1} c_{i,k} e^{2jf_k t} \quad (25)$$

Where $f_k = f_0 + \frac{k}{T_c}$, N_u is the user number and N_p is the number of subcarriers.
The optimum space between two adjacent subcarriers is equal to inverse of duration T_c of chip of spreading code in order to guarantee the orthogonality between subcarriers.

We assumed that the channel is time invariant and its impulse response is characterized by P paths of magnitudes β_p and phases θ_p. the impulse response is given by the following equation

$$h(\tau) = \sum_{p=0}^{P-1} \beta_p e^{\theta_p} \delta(\tau - \tau_p) \quad (26)$$

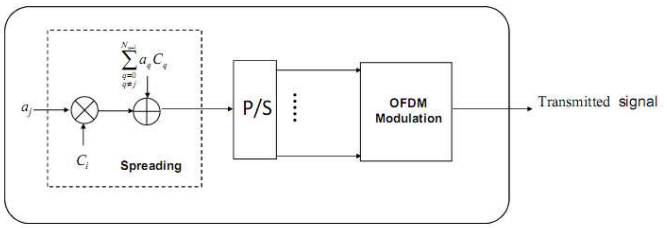

Fig. 3. The transmitter for downlink MC-CDMA systems

The relationship between the emitted signal $x(t)$ and the received signal $r(t)$ is given by:

$$\begin{aligned} r(t) &= \int_{-\infty}^{+\infty} \sum_{p=0}^{P-1} \beta_p e^{\theta_p} \delta(\tau - \tau_p) x(t-\tau) d\tau + n(t) \\ &= \sum_{p=0}^{P-1} \beta_p e^{\theta_p} x(t-\tau_p) + n(t) \end{aligned} \tag{27}$$

Where $n(t)$ is an additive white Gaussian noise (AWGN).

B. MC−CDMA Receiver

The downlink received MC−CDMA signal at the input receiver is given by the following equation

In Figure 4 we represent the receiver for downlink MC-CDMA systems.

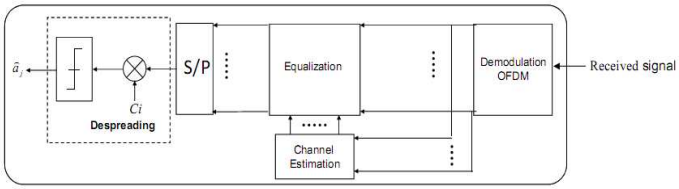

Fig. 4. The receiver for downlink MC-CDMA systems

$$\begin{aligned} r(t) = \frac{1}{\sqrt{N_p}} \sum_{p=0}^{P-1} \sum_{k=0}^{N_p-1} \sum_{i=0}^{N_u-1} \times \\ \times Re\Big\{ \beta_p e^{j\theta} a_i c_{i,k} e^{2j\pi(f_0 + k/T_c)(t-\tau_p)} \Big\} + n(t) \end{aligned} \tag{28}$$

At the reception, we demodulate the signal according the N_p subcarriers, and then we multiply the received sequence by the code of the user. After the equalization and the spreading operation, the estimation $\widehat{a_i}$ of the emitted user symbol a_i, of the i^{th} user can be written by the following equation

$$\begin{aligned} \widehat{a_i} &= \sum_{q=0}^{N_u-1} \sum_{k=0}^{N_p-1} c_{i,k}(g_k h_k c_{q,k} a_q + g_k n_k) \\ &= \underbrace{\sum_{k=0}^{N_p-1} c_{i,k}^2 (g_k h_k a_i)}_{I \quad (i=q)} \\ &+ \underbrace{\sum_{q=0}^{N_u-1} \sum_{k=0}^{N_p-1} c_{i,k} c_{q,k} g_k h_k a_q}_{II \quad (i \neq q)} \\ &+ \underbrace{\sum_{k=0}^{N_p-1} c_{i,k}(g_k n_k)}_{III} \end{aligned} \tag{29}$$

C. Equalization for MC−CDMA

1) Zero forcing (ZF): The principle of the ZF, is to completely cancel the distortions brought by the channel. The gain factor of the ZF equalizer,is given by the equation

$$g_k = \frac{1}{|h_k|} \tag{30}$$

By that manner, each symbol is multiplied by a unit magnitude. So, the estimated received symbol, $\widehat{a_i}$ of symbol a_i of the user i is described by:

$$\widehat{a_i} = \underbrace{\sum_{k=0}^{N_p-1} c_{i,k}^2 a_i}_{I \quad (i=q)} + \underbrace{\sum_{q=0}^{N_u-1} \sum_{k=0}^{N_p-1} c_{i,k} c_{q,k} a_q}_{II \quad (i \neq q)} + \underbrace{\sum_{k=0}^{N_p-1} c_{i,k} \frac{1}{h_k} n_k}_{III} \tag{31}$$

If we suppose that the spreading code are orthogonal, $i.e.$,

$$\sum_{k=0}^{N_p-1} c_{i,k} c_{q,k} = 0 \qquad \forall i \neq q \tag{32}$$

Eq. (31) will become

$$\widehat{a_i} = \sum_{k=0}^{N_p-1} c_{i,k}^2 a_i + \sum_{k=0}^{N_p-1} c_{i,k} \frac{1}{h_k} n_k \tag{33}$$

2) Minimum Mean Square Error, (MMSE): The MMSE techniques minimize the mean square error for each subcarrier k between the transmitted signal x_k and the output detection

$$E[|\varepsilon|^2] = E[|x_k - g_k r_k|^2] \tag{34}$$

The minimization of the function $E[|\varepsilon|^2]$, gives us the optimal equalizer coefficient, under the minimization of the mean square error criterion, of each subcarrier as

$$g_k = \frac{h_k^*}{|h_k|^2 + \frac{1}{\zeta_k}} \tag{35}$$

Where $\zeta_k = \frac{E[|r_k h_k|^2]}{E[|n_k|^2]}$
The estimated received symbol, $\widehat{a_i}$ of symbol a_i of the user i is described by

$$\widehat{a_i} = \underbrace{\sum_{k=0}^{N_p-1} c_{i,k}^2 \frac{|h_k|^2}{|h_k|^2 + \frac{1}{\zeta_k}} a_i}_{I \quad (i=q)} + \underbrace{\sum_{q=0}^{N_u-1} \sum_{k=0}^{N_p-1} c_{i,k} c_{q,k} \frac{|h_k|^2}{|h_k|^2 + \frac{1}{\zeta_k}} a_q}_{II \quad (i \neq q)} + \underbrace{\sum_{k=0}^{N_p-1} c_{i,k} \frac{h_k^*}{|h_k|^2 + \frac{1}{\zeta_k}} n_k}_{III} \tag{36}$$

The same, if we suppose that the spreading code are orthogonal, $i.e.$,

$$\sum_{k=0}^{N_p-1} c_{i,k} c_{q,k} = 0 \qquad \forall i \neq q \tag{37}$$

Eq.(36) will become

$$\widehat{a_i} = \sum_{k=0}^{N_p-1} c_{i,k}^2 \frac{|h_k|^2}{|h_k|^2 + \frac{1}{\zeta_k}} a_i + \sum_{k=0}^{N_p-1} c_{i,k} \frac{h_k^*}{|h_k|^2 + \frac{1}{\zeta_k}} n_k \tag{38}$$

VI. Simulation results

In order to evaluate the performance of the proposed algorithm, we consider the BRAN A, BRAN B and BRAN D model representing the fading radio channels, the data corresponding to this model are measured for multicarrier code division multiple access (MC−CDMA) systems. The following equation describes the impulse response $h(k)$ of BRAN radio channel.

$$h(k) = \sum_{i=0}^{N_T} A_i \delta(k - \tau_i) \tag{39}$$

Where $\delta(k)$ is Dirac function, h_i the magnitude of the targets i, $N_T = 18$ the number of target and τ_i is the time delay (from the origin) of target i.
In order to estimates the parameters constituting the BRAN channels impulse response with maximum information, because the BRAN channels is constituted by $N_T = 18$ parameters and seeing that the latest parameters are very small, we have taking the following procedure:

- We decompose the BRAN channel impulse response into four sub-channel as follow:

$$h(k) = \sum_{j=1}^{3} h_j(k) \tag{40}$$

- We estimate the parameters of each sub-channel independently, using the proposed algorithm.

- We add all sub channel parameters, to construct the full BRAN C channel impulse response.

A. Bran A radio channel

In Table 1 we have summarized the values corresponding the BRAN A radio channel impulse response [14].

Delay $\tau_i[ns]$	Mag.$A_i[dB]$	Delay $\tau_i[ns]$	Mag.$A_i[dB]$
0	0	90	−7.8
10	−0.9	110	−4.7
20	−1.7	140	−7.3
30	−2.6	170	−9.9
40	−3.5	200	−12.5
50	−4.3	240	−13.7
60	−5.2	290	−18
70	−6.1	340	−22.4
80	−6.9	390	−26.7

Table 1: Delay and magnitudes of 18 targets of BRAN A channel

In Figure 5 we represent the estimation of the impulse response of BRAN A channel using the proposed and safi et al. algorithms in the case of SNR = 20 dB and data length N = 4096.

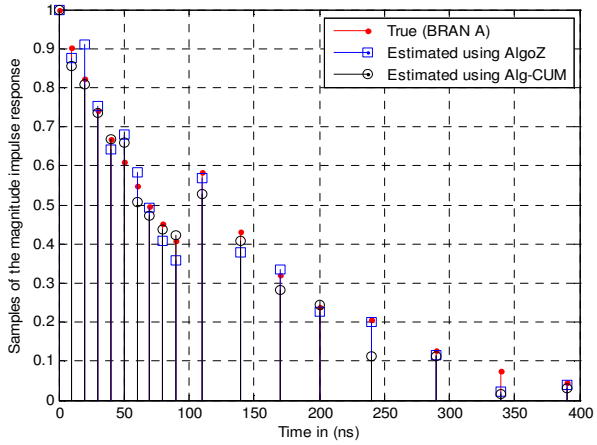

Fig. 5. Estimated of the BRAN A channel impulse response, for an SNR = 20 dB and a data length N=4096.

From Figure 5, we can conclude that the estimated BRAN A channel impulse response, using the proposed algorithm (AlgoZ), is very closed to the true one, for data length $N = 4096$ and $SNR = 20dB$. If we observe the estimated values of BRAN A impulse response, using the Safi et al. algorithm (Alg−CUM) shown in Figure 5, we remark, the same results given by the proposed method.
In the following figure (fig. 6) we have represented the estimated magnitude and phase of the impulse response BRAN A using all target, for an data length $N = 4096$ and $SNR = 20dB$, obtained using proposed algorithm (AlgoZ), compared with the safi et al. algorithm (Alg−CUM).

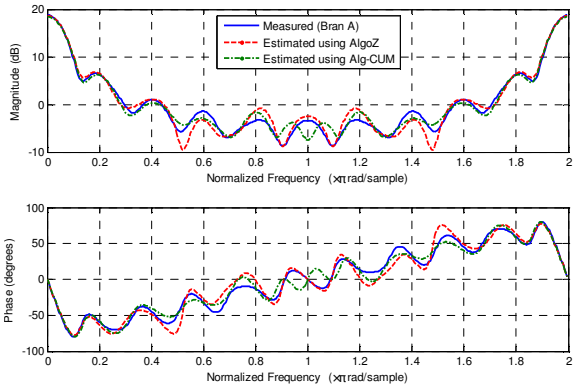

Fig. 6. Estimated of the BRAN A channel impulse response using all target, for an $SNR = 20dB$ and a data length N=4096

B. Bran B radio channel

In Table 2 we have represented the values corresponding to the BRAN B radio channel impulse response [14].

Delay $\tau_i[ns]$	Mag.$A_i[dB]$	Delay $\tau_i[ns]$	Mag.$A_i[dB]$
0	-2.6	230	-5.6
10	-3.0	280	-7.7
20	-3.5	330	-9.9
30	-3.9	380	-12.1
50	0.0	430	-14.3
80	-1.3	490	-15.4
110	-2.6	560	-18.4
140	-3.9	640	-20.7
180	-3.4	730	-24.6

Table 2: Delay and magnitudes of 18 targets of BRAN B channel

In Figure 7 we represent the estimation of the impulse response of BRAN B channel using the (AlgoZ) and (Alg$-$CUM) algorithms in the case of $SNR = 20dB$ and data length $N = 4096$.

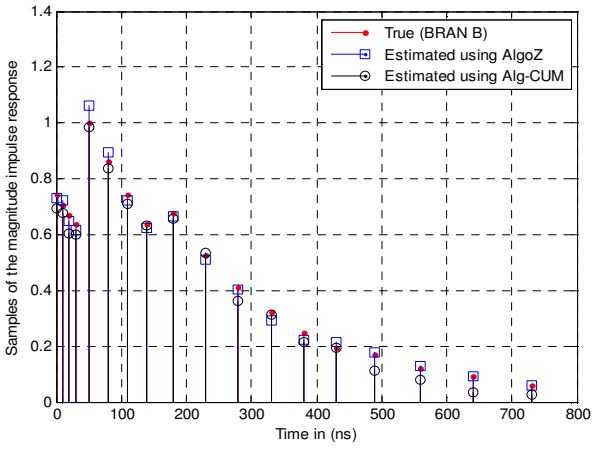

Fig. 7. Estimated of the BRAN B channel impulse response, for an $SNR = 20dB$ and a data length $N = 4096$.

From Figure 7, we can conclude that the estimated BRAN B channel impulse response, using (AlgoZ) algorithm, is very closed to the true one, for data length $N = 4096$ and $SNR = 20dB$. Using the algorithm (Alg$-$CUM) shown in Figure 7, we remark, approximately, the same results given by the AlgoZ except the last four parameters we have a minor difference between the estimated and the measured ones.

In the following figure (fig. 8) we have represented the estimated magnitude and phase of the impulse response BRAN B using all target, for an data length $N = 4096$ and $SNR = 20dB$, obtained using (AlgoZ) algorithm, compared with the Safi et al. algorithm (Alg$-$CUM).

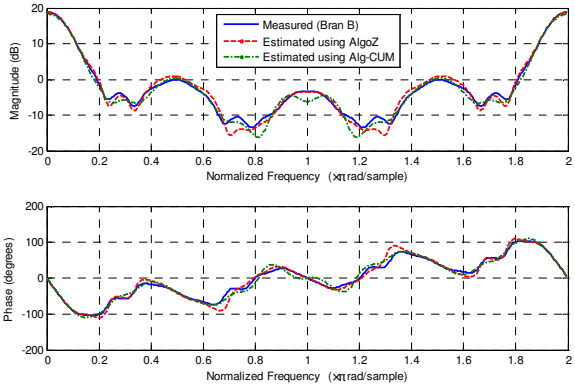

Fig. 8. Estimated of the BRAN B channel impulse response using all target, for an SNR = 20 dB and a data length N=4096

From the figure 8 we observe that the estimated magnitude and phase, using (AlgoZ) and (Alg$-$CUM) algorithms, have the same form and we have not more difference between the estimated and the true ones.

C. Bran D radio channel

In Table 3 we have represented the values corresponding to the BRAN D radio channel impulse response [14].

Delay $\tau_i[ns]$	Mag.$A_i[dB]$	Delay $\tau_i[ns]$	Mag.$A_i[dB]$
0	0.0	230	-9.4
10	-10.0	280	-10.8
20	-10.3	330	-12.3
30	-10.6	400	-11.7
50	-6.4	490	-14.3
80	-7.2	600	-15.8
110	-8.1	730	-19.6
140	-9.0	880	-22.7
180	-7.9	1050	-27.6

Table 3: Delay and magnitudes of 18 targets of BRAN D channel

In time domain we have represented the BRAN D channel impulse response parameters (Fig. 9)

From the gure (Fig. 9) we ca can conclude that the estimated BRAN D channel impulse response, using (AlgoZ) and (Alg$-$CUM), are very closed to the true ones, principally for high data length $(N = 4096)$, and for $SNR \geq 20dB$.

In the following figure (Fig. 10) we have represented the estimated magnitude and phase of the impulse response BRAN

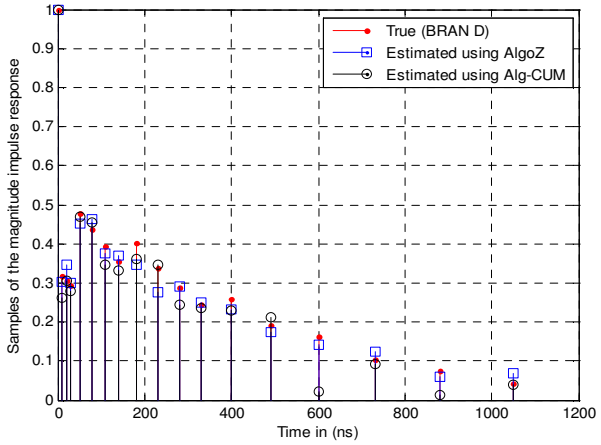

Fig. 9. Estimated of the BRAN D channel impulse response, for an SNR = 20 dB and a data length N=4096.

D using all target for an $N = 4096$ and $SNR = 20dB$.

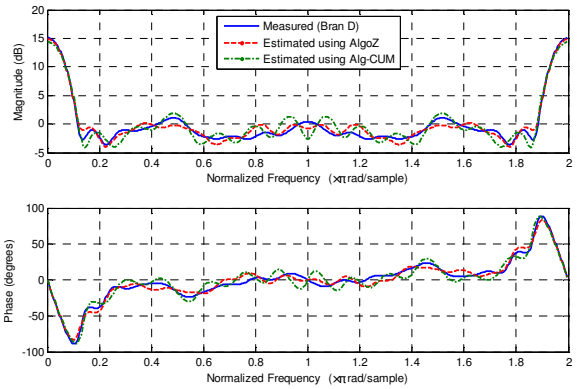

Fig. 10. Estimated of the BRAN D channel impulse response, for an SNR = 20 dB and a data length N=4096

From the gure 10 we observe that the estimated magnitude and phase, using (AlgoZ), have the same form between the estimated and the true ones, but using (Alg−CUM) we remark a faible difference between the estimated and the true ones.

VII. M-CDMA SYSTEM PERFORMANCE

In this subsection we consider the BER, for the two equalizers ZF and MMSE, using measured and estimated BRAN A, BRAN B, and BRAN D channel impulse responses.

A. ZF and MMSE Equalizers: Case of BRAN A Channel

In Figure 11, we represent the BER for different SNR, obtained using proposed algorithm (AlgoZ), compared with the (Alg−CUM) algorithm, using the ZF equalizer.

Figure 12 represents the BER for different SNR, obtained using proposed algorithm (AlgoZ), compared with the (Alg−CUM) algorithm, using the MMSE equalizer.

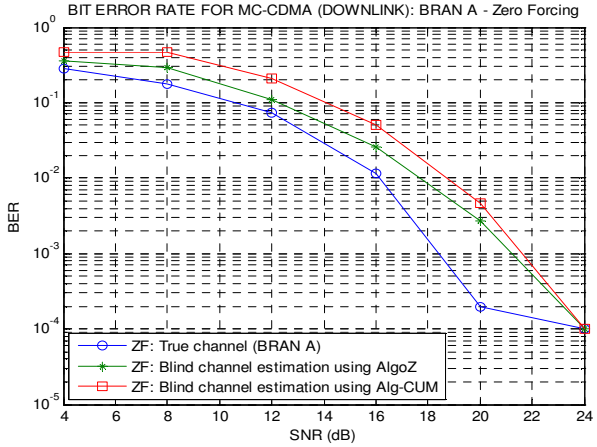

Fig. 11. BER of the estimated and measured BRAN A channel using the ZF equalizer

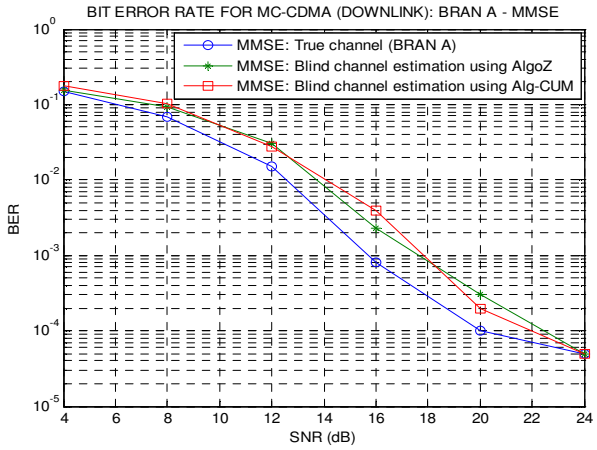

Fig. 12. BER of the estimated and measured BRAN A channel using the MMSE equalizer.

The BER simulation for different SNR, demonstrates that the estimated values by the (AlgoZ) algorithm are more close to the measured value than those estimated by (Alg−CUM) algorithm, we have a faible difference, for ZF and MMSE equalization. From the figure 12, we conclude that: if the SNR=24dB we have 1 bit error occurred when we receive 10^5 bit using MMSE equalizer.

B. ZF and MMSE Equalizers: Case of BRAN B Channel

In Figure 13, we represent the BER for different SNR, obtained using proposed algorithm (AlgoZ), compared with the (Alg−CUM) algorithm, using the ZF equalizer.

Figure 14 represents the BER for different SNR, obtained using proposed algorithm (AlgoZ), compared with the (Alg−CUM) algorithm, using the MMSE equalizer.

The BER simulation for different SNR, demonstrates that the estimated values by the (AlgoZ) algorithm are more close to the measured value than those estimated by (Alg−CUM) algorithm. From the figure 14, we conclude that: if the

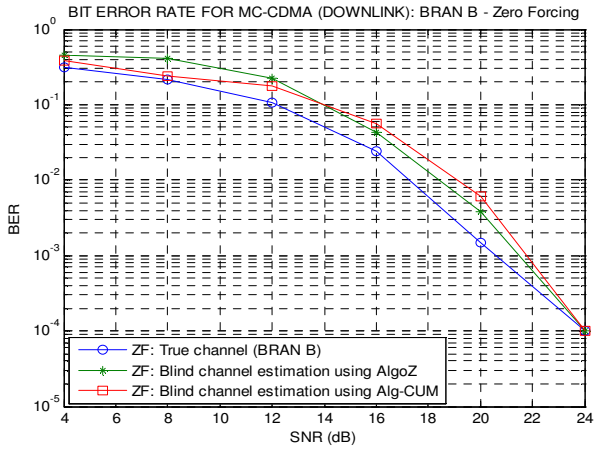

Fig. 13. BER of the estimated and measured BRAN B channel using the ZF equalizer.

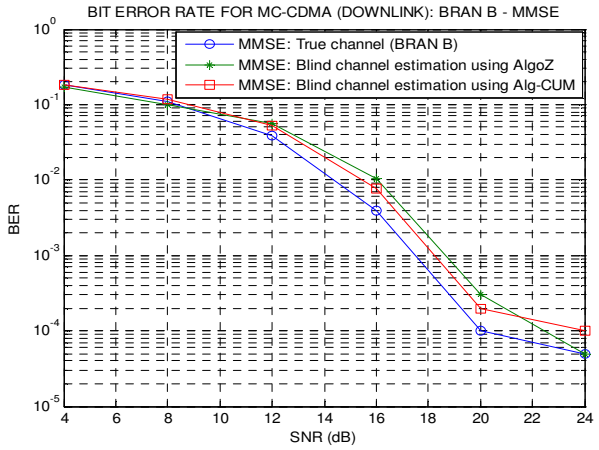

Fig. 14. BER of the estimated and measured BRAN B channel using the MMSE equalizer

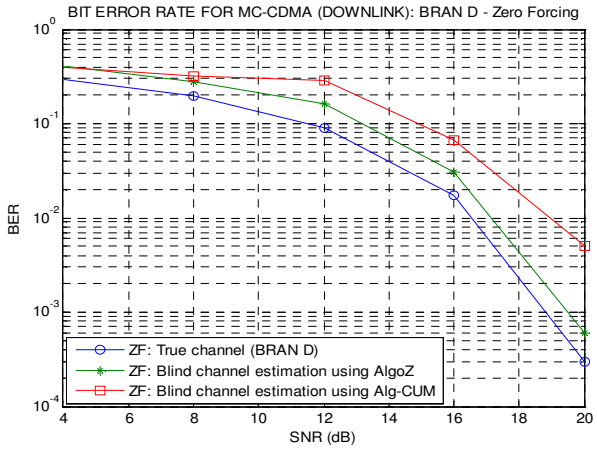

Fig. 15. BER of the estimated and measured BRAN D channel using the ZF equalizer

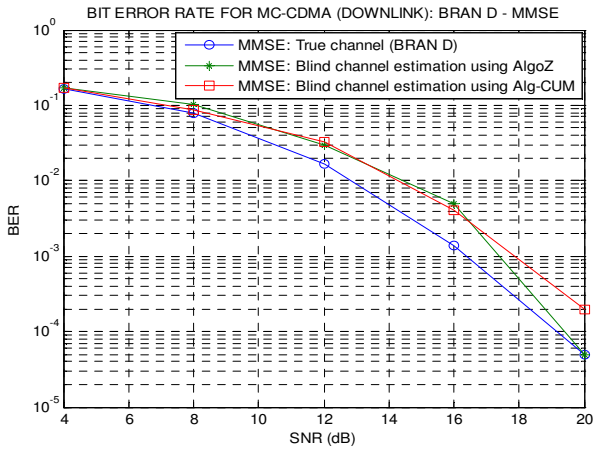

Fig. 16. BER of the estimated and measured BRAN D channel using the MMSE equalizer

$SNR = 24dB$, we observe that 1 bit error occurred when we receive 10^4 bit with the (Alg−CUM), but using (AlgoZ) we obtain only one bit error for 10^5 bit received.

C. ZF and MMSE Equalizers: Case of BRAN D Channel

In the figure 15, we represent the BER for different SNR, using the measured and estimated BRAN D channel, using the ZF equalizer.

From the figure 15, we observe that the blind ZF equalization gives approximately the same results obtained by the measured BRAN D values using AlgoZ, than those obtained by (Alg−CUM) algorithm, we have a difference between the estimated and the measured ones. If the $SNR = 20dB$ we have a BER less than 10^{-3} using (AlgoZ), but using the (Alg−CUM) we have only the BER less than 10^{-2}.

Figure 16 represents the BER for different SNR, using the measured and estimated BRAN D channel, using the MMSE equalizer.

Figure 16 demonstrates clearly that the estimated values by the rst algorithm (AlgoZ) are close to the measured value than those estimated by second algorithm (Alg−CUM), So, if the $SNR = 20dB$, we observe that 1 bit error occurred when we receive 10^4 bit with the (Alg−CUM), but using (AlgoZ) we obtain only one bit error for 10^5 bit received.

VIII. Conclusion

In this paper we have proposed an new algorithm (AlgoZ) based on fourth order cumulants, compared with the Safi et al algorithm (Alg−CUM), to identify the parameters of the impulse response of the frequency selective channel such as the experimental channels, BRAN A, BRAN B, and BRAN D, normalized for MC−CDMA systems. The simulation results show the effciency of the proposed algorithm (AlgoZ) than those obtained using (Alg−CUM), mainly if the input data are suffcient. The magnitude and phase of the impulse response is estimated with an acceptable precision in noisy environment principally if we use the rst algorithm (AlgoZ). In part of three experimental channels for MC−CDMA systems application, we have obtained very important results on bit error rate using the proposed algorithm (AlgoZ), than those obtained by (Alg−CUM) algorithm.

REFERENCES

[1] L. Srinivas and K. V. S. Hari, "FIR System Identification Based on Subspaces of a Hight Order Cumulant Matrix", IEEE Transactions on signal processing, 44(6) (1996).

[2] S. Safi, M. Frikel, M. M'Saad and A. Zeroual, "Blind Impulse Response Identification of frequency Radio Channels: Application to Bran A Channel", Int. J. Sig. Proces., 4(1) 201-206 (2007).

[3] M. Bakrim and D. Aboutajdine, "Cumulant-based identification of non gaussian moving average signals", Traitement du Signal, 16(3) 175-186 (1999).

[4] S. Safi and A. Zeroual, "Blind non-minimum phase channel identification using 3^{rd} and 4^{th} order cumulants", Int. J. Sig. Proces., 4 (1), 158-168 (2008).

[5] C.Y. Chi and J.Y. Kung, "A new identification algorithm for allpass systems by higher-order statistics", Signal Processing 41 239- 256 (1995).

[6] J. Antari, A. El Khadimi, D. Mammas and A. Zeroual, "Developed Algorithm for Supervising Identification of Non Linear Systems using Higher Order Statistics: Modeling Internet Traffic", International Journal of Future Generation Communication and Networking, 5(4) (2012).

[7] J. Antari, A. Zeroual and S. Safi, "Stochastic analysis and parametric identification of moving average (MA) non Gaussian signal using cumulants", International Journal of Physical and Chemical News, 34 27-32 (2007).

[8] K. Abderrahim, R. B. Abdennour, G. favier, M. Ksouri and F. Msahli, "New results on FIR system identification using cumulants", 35 601-622 (2001).

[9] S. Safi, A. Zeroual and M. M. Hassani, "Prediction of global daily solar radiation using higher order statistics" Renewable Energy, 27 647666 (2002).

[10] S. Safi and A. Zeroual, "Blind identification in noisy environment of non-minimum phase Finite Impulse Response (FIR) using higher order statistics", Int. J. Sys. Anal. Modell. Simul., Taylor Francis, 43(5) 671681 (2003).

[11] J. Antari, R. Iqdour, A. Zeroual, "Forecasting the wind speed process using higher order statistics and fuzzy systems", Renewable Energy, 9 237 251 (2006).

[12] ETSI, "Broadband Radio Access Networks (BRAN), High Performance Radio Logical Area Network (HIPERLAN) Type 2; Requirements and architectures for wireless broadband access" (1999).

[13] ETSI, "Broadband Radio Access Networks (BRAN); HIPERLAN Type 2; Physical Layer" (2001).

[14] Vincent Le Nir, "Étude et optimisation des systèmes multi-antennes associés à des modulations multiporteuses", Thèse de doctorat, Institut National des Sciences Appliquées de Rennes, (2004).